Table 4.8: Statistical summary of concentrations of iron, nickel, potassium, strontium, rubidium, and zirconium (continued).

(f) ZIRCONIUM (ng/m^3)

SITE	NO. of OBS	STD DEV	MAX	90th PRCNTL	75th PRCNTL	MEAN	MED	MIN
WUPATKI	43	0.3100	1.4000	0.7000	0.0000	0.1200	0.0000	0.0000
HITE	80	0.2600	1.0600	0.5900	0.0000	0.1100	0.0000	0.0000
NAVAJO	42	0.2400	0.9000	0.6000	0.0000	0.1000	0.0000	0.0000
HOPI POINT	81	0.1700	0.5000	0.3900	0.0000	0.0900	0.0000	0.0000
MONTICELLO	72	0.2000	0.8300	0.4600	0.0000	0.0800	0.0000	0.0000
PAGE	83	0.1700	0.6000	0.3900	0.0000	0.0800	0.0000	0.0000
BRYCE CANYON	39	0.2700	1.1000	0.0000	0.0000	0.0700	0.0000	0.0000
BULLFROG	82	0.1700	0.8200	0.4000	0.0000	0.0700	0.0000	0.0000
CANYONLANDS	82	0.1600	0.7500	0.3500	0.0000	0.0700	0.0000	0.0000
GREEN RIVER	81	0.2300	1.1000	0.4700	0.0000	0.0700	0.0000	0.0000
MEXICAN HAT	71	0.2300	1.0700	0.3400	0.0000	0.0700	0.0000	0.0000
CISCO	44	0.2100	0.9000	0.2800	0.0000	0.0600	0.0000	0.0000
MEADVIEW	13	0.5620	0.3890	0.3890	0.1640	−.4070	−.5410	−.9340

Relative humidity apparently plays an important role in the conversion of SO_2 to sulfates; when the relative humidity is high many conversion processes are either triggered or accelerated causing non-linear relationships between predictor variables and sulfate concentrations. One mathematical way of treating this non-linearity is to multiply predictor variables by the relative humidity. Table 4.9 has the statistical summaries of three tracers multiplied by relative humidity; the tracers are CD_4, selenium, and arsenic.

4.5 Temporal History of Meteorological Data

Figures 4.18 through 4.21 shows the temporal history of extinction, scattering, temperature, relative humidity, wind speed, and wind direction for the three major sites (Canyonlands, Page, and Hopi) and Bullfrog. At Page (Figure 4.18), the meteorological aspects of the episode are evident. The episode begins on JD=41; the winds for several days preceding are light and variable, and the wind directions show a clear diurnal pattern alternating between north at day and south at night, indicating stagnant conditions. The episode is triggered by a dramatic change in the relative humidity; on day 41 through day 44 the relative humidity stays consistently in the range of 85% - 98%, whereas before the episode the humidity is around 35% - 45%. High humidity affects visibility in two ways: first, sulfate production is enhanced; and secondly, the deliquescence point for sulfate aerosol is around 70%. During the episode the amplitude of the diurnal variation of temperature is clearly dampened. Termination of the episode is indicated by a dramatic increase in wind speed, loss of the diurnal wind pattern, and a sudden drop in humidity to around 30% on JD=45.

The other three sites (Figures 4.19 - 4.21) show similar regimes during the episode. However, two of these sites, Hopi and Canyonlands, experience many periods of high relative humidity. Table 4.10 lists the days that precipitation was recorded at the Grand Canyon NOAA weather monitoring station, these days coincide with the times that the transmissometer data are missing at Hopi. Nevertheless, at Hopi, the high relative humidity times are accompanied by increases in scattering.

Table 4.9: Statistical summary of the tracers CD_4, selenium, and arsenic ($\mu g/m^3$) multiplied by relative humidity (RH - %)

(a) SCALED $CD_4 * RH$ (ppt * %)

SITE	NO. of OBS	STD DEV	MAX	90th PRCNTL	75th PRCNTL	MEAN	MED	MIN
PAGE	32	0.6348	3.4412	0.7071	0.4854	0.4019	0.2855	0.0000
HOPI POINT	36	0.1136	0.4484	0.2955	0.2655	0.1605	0.1364	0.0171

(b) $As * RH$ ($\mu g/m^3$ * %)

SITE	NO. of OBS	STD DEV	MAX	90th PRCNTL	75th PRCNTL	MEAN	MED	MIN
PAGE	83	0.0828	0.4590	0.1655	0.1035	0.0717	0.0503	0.0000
CISCO	44	0.0638	0.2492	0.1371	0.0922	0.0537	0.0398	0.0000
GREEN RIVER	81	0.0529	0.2316	0.1272	0.0870	0.0508	0.0357	0.0000
MONTICELLO	72	0.0592	0.2673	0.1237	0.0729	0.0398	0.0000	0.0000
BULLFROG	65	0.0358	0.1792	0.0751	0.0470	0.0283	0.0179	0.0000
CANYONLANDS	82	0.0200	0.0735	0.0468	0.0333	0.0196	0.0193	0.0000
HOPI POINT	79	0.0394	0.1699	0.0823	0.0158	0.0194	0.0000	0.0000
HITE	80	0.0230	0.1427	0.0365	0.0158	0.0112	0.0000	0.0000
BRYCE CANYON	39	0.0076	0.0325	0.0000	0.0000	0.0021	0.0000	0.0000

(c) $Se * RH$ ($\mu g/m^3$ * %)

SITE	NO. of OBS	STD DEV	MAX	90th PRCNTL	75th PRCNTL	MEAN	MED	MIN
PAGE	83	0.0361	0.1774	0.0747	0.0545	0.0330	0.0270	0.0000
CISCO	44	0.0429	0.1953	0.1078	0.0393	0.0289	0.0117	0.0000
BULLFROG	65	0.0308	0.1567	0.0670	0.0432	0.0282	0.0209	0.0000
GREEN RIVER	81	0.0498	0.2183	0.1050	0.0442	0.0277	0.0000	0.0000
CANYONLANDS	82	0.0150	0.0512	0.0341	0.0173	0.0100	0.0000	0.0000
HOPI POINT	77	0.0082	0.0371	0.0212	0.0141	0.0090	0.0075	0.0000
MONTICELLO	72	0.0165	0.0640	0.0385	0.0000	0.0082	0.0000	0.0000
HITE	80	0.0151	0.0658	0.0347	0.0100	0.0076	0.0000	0.0000
BRYCE CANYON	39	0.0092	0.0325	0.0193	0.0000	0.0035	0.0000	0.0000

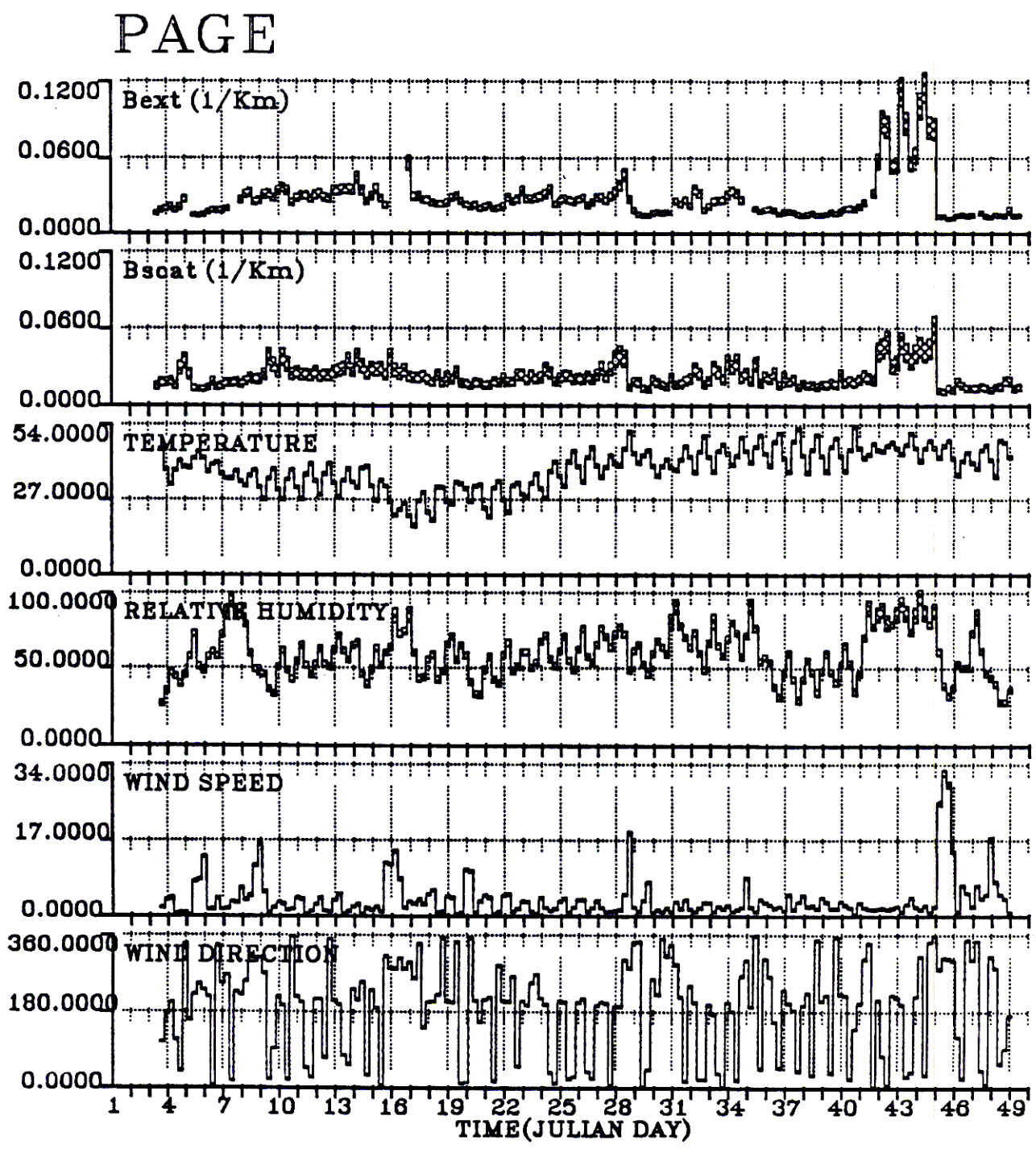

Figure 4.18: Temporal history of extinction, scattering, temperature, relative humidity, wind speed, and wind direction at Page.

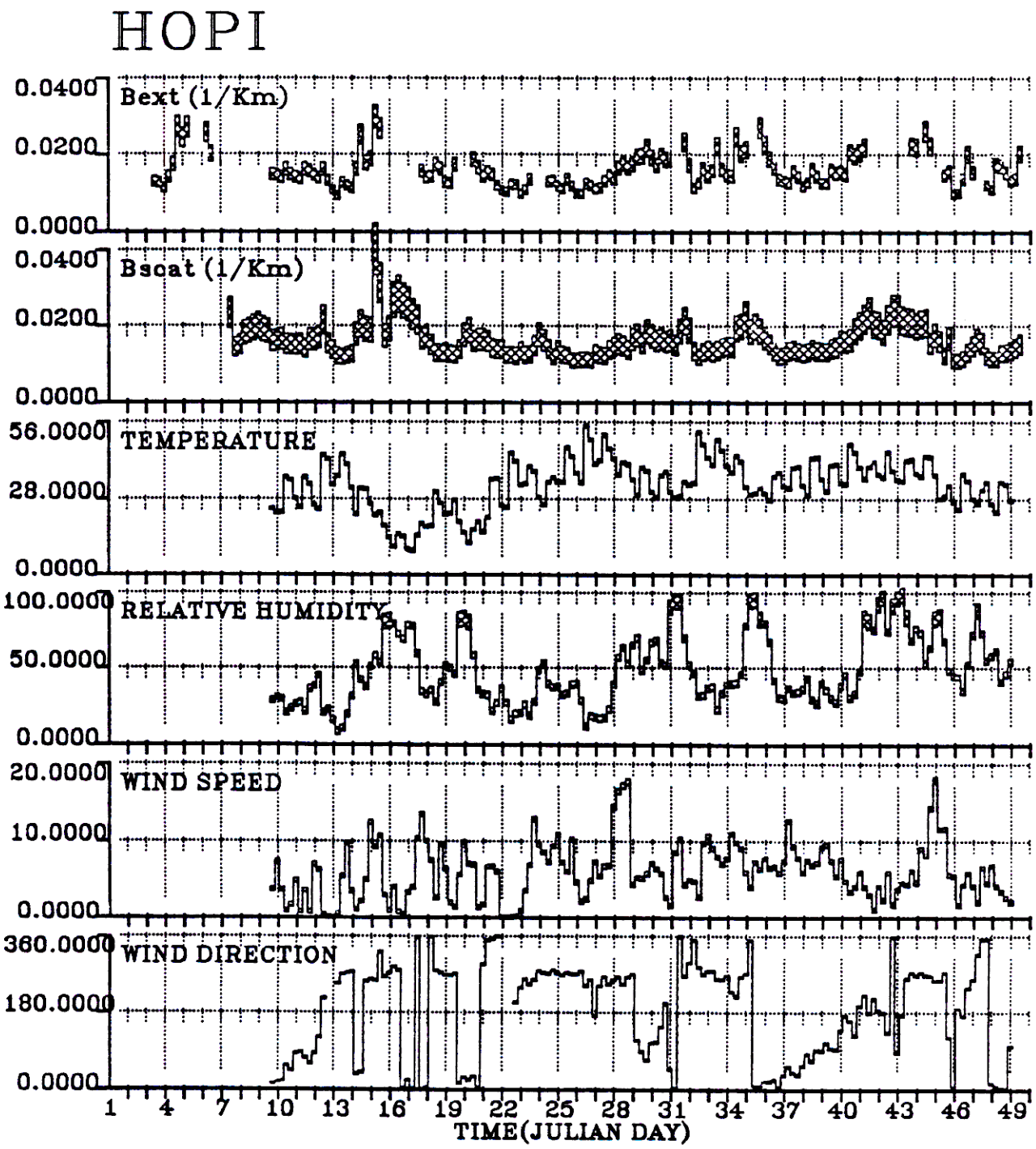

Figure 4.19: Temporal history of extinction, scattering, temperature, relative humidity, wind speed, and wind direction at Hopi.

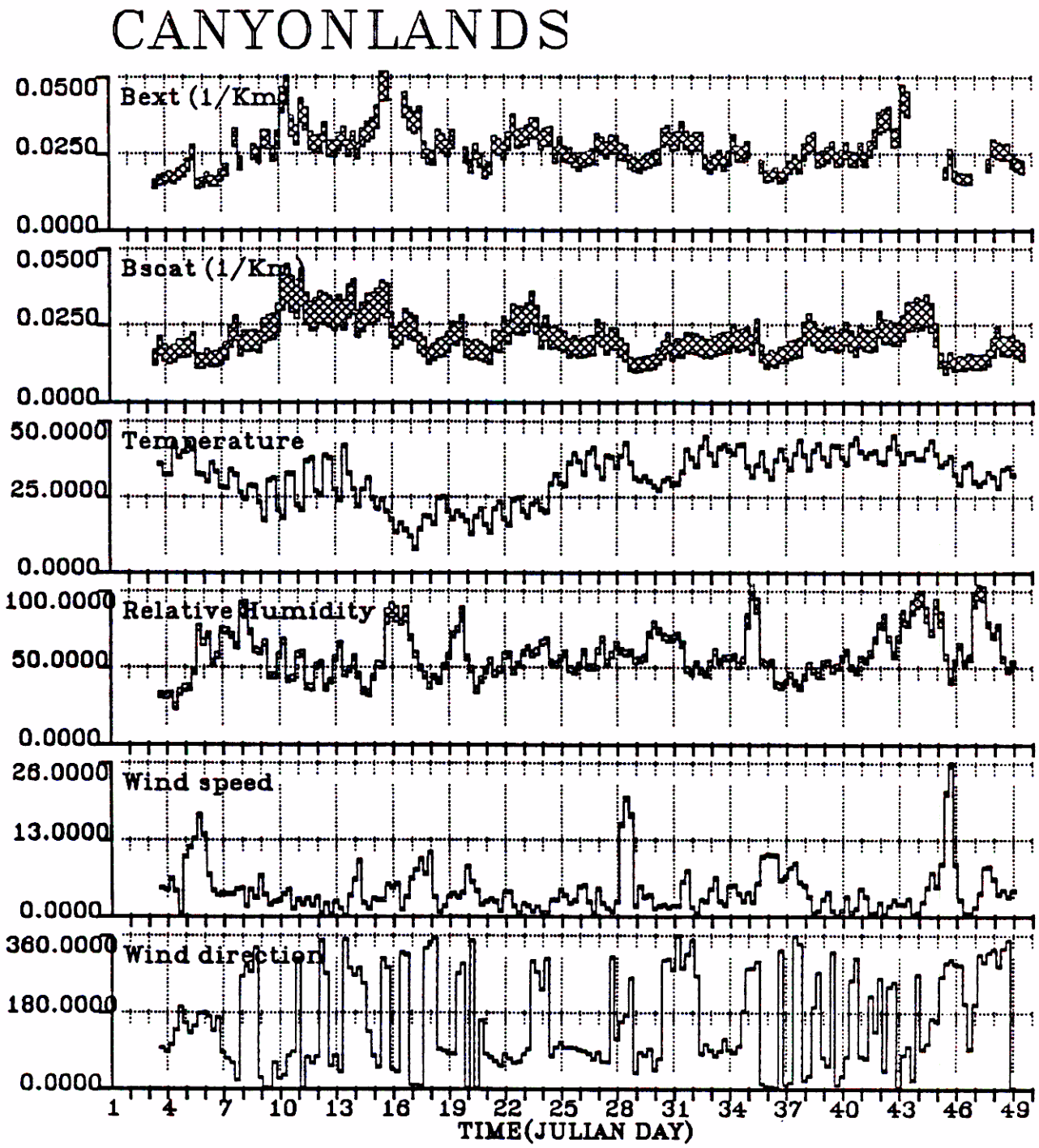

Figure 4.20: Temporal history of extinction, scattering, temperature, relative humidity, wind speed, and wind direction at Canyonlands.

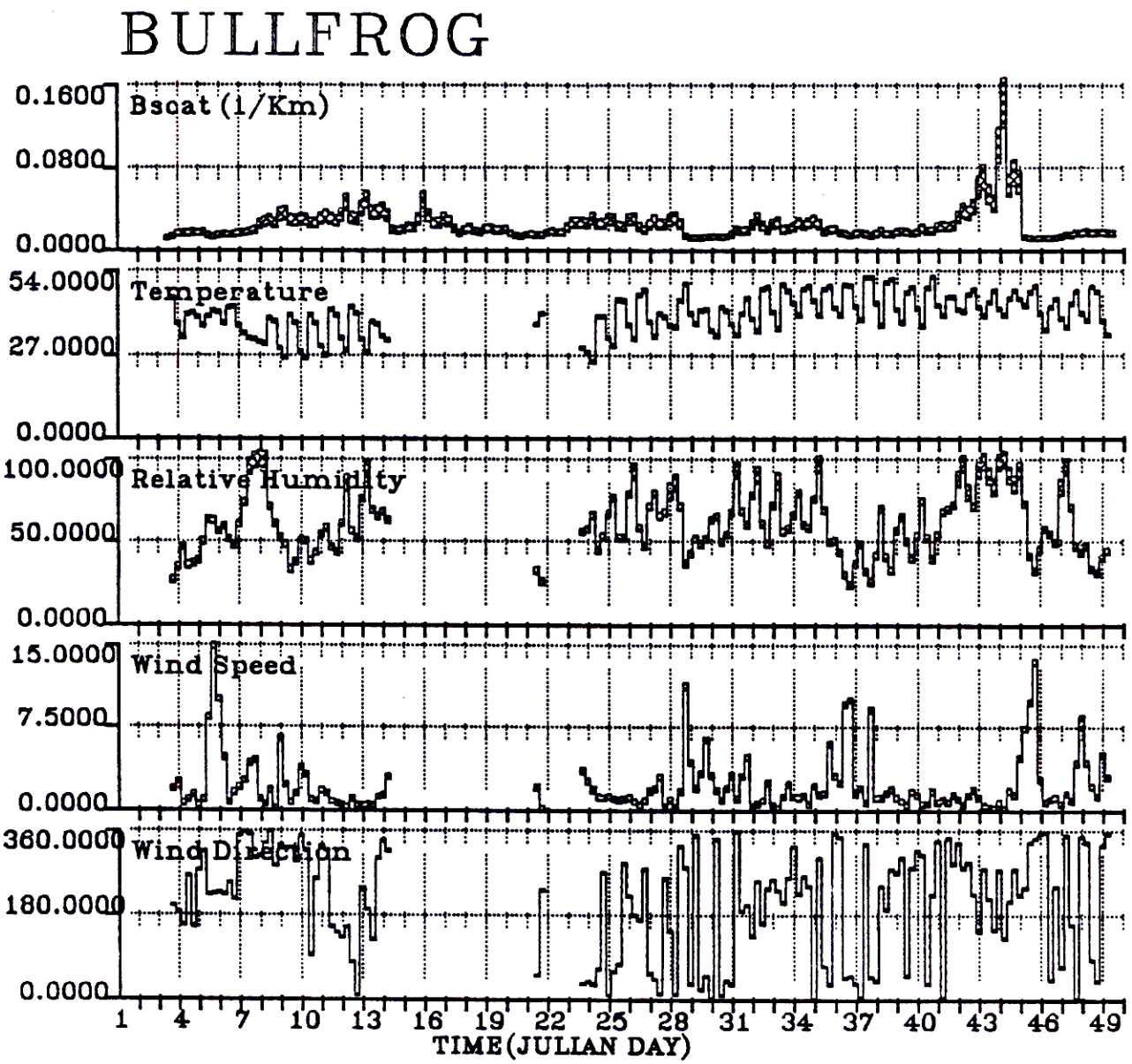

Figure 4.21: Temporal history of scattering, temperature, relative humidity, wind speed, and wind direction at Bullfrog.

Table 4.10: Daily precipitation in inches at Hopi as reported by the NOAA Grand Canyon weather monitoring station.

Jan 1	t	Feb 1	.01
Jan 2	t	Feb 4	.18
Jan 3	t	Feb 10	.09
Jan 4	t	Feb 11	.06
Jan 5	.35	Feb 12	.14
Jan 6	.16	Feb 14	.22
Jan 7	.05	Feb 16	t
Jan 8	.07	Feb 17	t
Jan 16	.03		
Jan 17	.02		
Jan 20	.08		
Jan 28	t		
Jan 29	.02		
Jan 31	.18		

What distinguishes the major mid-February episode are uniform meteorological conditions across the entire WHITEX study region. Figure 4.22 shows wind vectors on an hourly basis for the major and gradient sites on JD=43, a day of bad visibility at Page, Hopi, Canyonlands, Bullfrog and elsewhere. The winds are light and variable and exhibit a diurnal "sloshing" back and forth indicating stagnant conditions. The episode is abruptly terminated before dawn on JD=45 by the passage of a strong front as Figure 4.23 shows. This episode varies considerably with other minor episodes that occurred during the WHITEX period. For example, Figure 4.24 shows the wind vectors on JD=28, a day of impaired visibility at Bullfrog and Page, conditions are stagnant at Bullfrog and Page until noon when a fast moving front cleans out the atmosphere. However, on JD=28, many sites are experiencing very windy conditions throughout the day; at Hopi, very high concentrations of fine soil and increased extinction were reported that afternoon.

Appendix 6E has daily wind vectors for all days of the WHITEX study period and Appendix 6F has plots of the upper air soundings. The upper air data were collected from soundings 3 times daily at 0600, 1100, and 1700 hours at Canyonlands and Page.

4.6 Relationships Between Variables

Insight into the relationships between primary emissions and their secondary byproducts can be gained by comparing the fully scaled CD_4 and trace element data with ammonium sulfate, ammonium nitrate, total sulfur, total nitrate nitrogen, and other components of fine mass. It is also of interest to examine relationships between trace elements, secondary aerosols and fully scaled CD_4 concentrations. Only at Page and Hopi Point are there an adequate number of CD_4 samples analyzed to scatter against the other data.

All data presented in this section that are not of 12 hour duration will be either averaged from 6 hour data to 12 hour data or disaggregated from 24 hour data to to 12 hour values. The 6 hour